New Phytologist

Research

Effects of kinetics of light-induced stomatal responses on photosynthesis and water-use efficiency

Lorna McAusland[1]*, Silvère Vialet-Chabrand[1]*, Philip Davey[1], Neil R. Baker[1], Oliver Brendel[2,3] and Tracy Lawson[1]

[1]School of Biological Sciences, University of Essex, Colchester, CO4 3SQ, UK; [2]INRA, UMR1137 'Ecologie et Ecophysiologie Forestières', F-54280 Champenoux, France; [3]UMR1137 'Ecologie et Ecophysiologie Forestières', Faculté des Sciences, Université de Lorraine, F-54500 Vandoeuvre-Les-Nancy, France

Author for correspondence:
Tracy Lawson
Tel: +44 (0)1206 873327
Email: tlawson@essex.ac.uk

Received: *8 January 2016*
Accepted: *24 March 2016*

New Phytologist (2016)
doi: 10.1111/nph.14000

Key words: guard cells, intrinsic water use efficiency, kinetics of stomatal responses, photosynthesis, stomatal conductance.

Summary

- Both photosynthesis (A) and stomatal conductance (g_s) respond to changing irradiance, yet stomatal responses are an order of magnitude slower than photosynthesis, resulting in noncoordination between A and g_s in dynamic light environments.
- Infrared gas exchange analysis was used to examine the temporal responses and coordination of A and g_s to a step increase and decrease in light in a range of different species, and the impact on intrinsic water use efficiency was evaluated.
- The temporal responses revealed a large range of strategies to save water or maximize photosynthesis in the different species used in this study but also displayed an uncoupling of A and g_s in most of the species. The shape of the guard cells influenced the rapidity of response and the overall g_s values achieved, with different impacts on A and W_i. The rapidity of g_s in dumbbell-shaped guard cells could be attributed to size, whilst in elliptical-shaped guard cells features other than anatomy were more important for kinetics.
- Our findings suggest significant variation in the rapidity of stomatal responses amongst species, providing a novel target for improving photosynthesis and water use.

Introduction

Stomata control the balance of gases between the internal leaf environment and the external atmosphere; regulating CO_2 uptake for photosynthesis and water loss through transpiration (E). Low stomatal conductance to water vapour (g_s) can restrict CO_2 uptake by limiting CO_2 influx and thus net CO_2 assimilation rate (A), whereas high g_s facilitates high rates of A, but greater water loss is an inevitable consequence.

This balance between CO_2 limitation and water loss is characterized by intrinsic water use efficiency (W_i), which is the ratio between A and g_s. On an instantaneous timescale, maintaining a suitable and appropriate balance is impeded by the temporal stomatal responses, which are a magnitude slower than those of A. Therefore, in response to changing light, the kinetics of g_s can greatly impact CO_2 uptake and water loss, which has significant implications water use efficiency (WUE). WUE can be defined as the ratio of net CO_2 uptake relative to water loss through transpiration (E) or as the ratio of biomass or yield accumulation to water use over the growing season. Consequently, WUE is often a target for improving crop performance; however, it should be noted that greater W_i is often at the expense of A (Blum, 2009; Lawson *et al.*, 2010; Lawson & Blatt, 2014). The rate of water transpired through the stomata is an order of magnitude greater than the rate of CO_2 uptake for A due to the greater water concentration gradient between the intercellular spaces within the leaf and the external atmosphere (as well as biochemical limitation on A). In order to maintain an optimal balance between A and E, stomatal guard cells are continually adjusting to environmental and intracellular cues (Lawson & Blatt, 2014).

Many previous studies have reported a strong correlation between A and g_s (Wong *et al.*, 1979; Farquhar & Sharkey, 1982). This correlation is generally observed because steady-state values are often reported, yet under dynamic conditions g_s responses are not always coupled with A (Knapp & Smith, 1987, 1990). In natural environments, photosynthetic photon flux density (PPFD) fluctuates on timescales of seconds to days and seasons (Assmann & Wang, 2001) driven by changes in cloud cover, sun angle and shading from adjacent leaves in the canopy (Pearcy, 1990; Chazdon & Pearcy, 1991; Way & Pearcy, 2012). Plants therefore experience short and long term fluctuations in PPFD creating 'sun' and 'shade' flecks to which A and g_s respond. Slower stomatal opening when A responds rapidly to a PPFD increase can limit CO_2 assimilation (Tinoco-Ojanguren & Pearcy, 1993), whilst delayed stomatal closing responses following a decrease in PPFD and photosynthesis result in unnecessary water loss when carbon gain is limited (Lawson *et al.*, 2010; Lawson & Blatt, 2014). Due to the difference in the rate of carbon gain to water loss, any disparity in the response of A and

*These authors contributed equally to this work.

© 2016 The Authors
New Phytologist © 2016 New Phytologist Trust
This is an open access article under the terms of the Creative Commons Attribution License, which permits use, distribution and reproduction in any medium, provided the original work is properly cited.

g_s also increases the probability of water stress (Condon *et al.*, 2002). For example, slow closing of stomata when A has decreased will result in higher than necessary transpiration rates that will deplete the soil water more rapidly and thus potentially create a soil water deficit.

It has been estimated that stomata can limit A by up to 20%, which can impact substantially on crop yields (Farquhar & Sharkey, 1982; Jones, 1987, 1998; Fischer *et al.*, 1998; Lawson & Blatt, 2014). In order to maximize A and optimize W_i, species or cultivars with rapid stomatal responses would be intuitively desirable, as there would be greater synchrony with mesophyll demands for CO_2. Amplitude and rapidity of stomatal movements are therefore potential targets to improve A and W_i. The majority of studies reporting stomatal influences on photosynthesis describe steady-state values and explore the potential of increasing or decreasing g_s to enhance A or diminish water loss, however this often results in an overall reduction of A and thus productivity (Blum,2009). We propose here to follow another approach for plant improvement, which exploits stomatal kinetics to facilitate synchronous g_s responses with mesophyll demands for CO_2, thus simultaneously reducing CO_2 limitations as well as avoidable water losses, incidentally enhancing W_i.

Only a handful of investigations have focused on dynamic stomatal responses and even fewer of these have explored the effects on A and W_i. Most of these studies have examined forest understorey species and the impact of sun-fleck regimes on A and E (Pearcy, 1990; Tinoco-Ojanguren & Pearcy, 1993; Leakey *et al.*, 2005; Way & Pearcy, 2012). In addition, assessing the rapidity of stomatal movements is complicated by variation in both the sensitivity and responsiveness of stomata between different species (Ooba & Takahashi, 2003; Lawson *et al.*, 2010; Vico *et al.*, 2011) and between individuals of the same species grown in different habitats (Drake *et al.*, 2013). After a change in PPFD, the temporal response of g_s is usually composed of three steps: an initial lag where the value of g_s remains stable for several minutes, followed by an exponential phase during which rapid increases in g_s are observed before reaching final steady-state plateau (Naumburg *et al.*, 2001; Vialet-Chabrand *et al.*, 2013). Recently, a dynamic sigmoidal model has been developed by Vialet-Chabrand *et al.* (2013) to analyse the temporal response of g_s by estimating the initial lag time (λ), a time constant (k) and a steady-state target (G_{smax}; see Table 1 for a summary of parameters and units). The time constant was used to describe the rapidity of the exponential phase independently of the amplitude of the g_s response, facilitating species or cultivar comparisons as well as proposing a more accurate interpretation.

In order to determine the impact of stomatal responses to increasing and decreasing PPFD on limitation of A, water loss and intrinsic WUE, we have assessed and quantified the rapidity of stomatal movements in a range of plant types, including several major crops. We have selected species with kidney- and dumbbell-shaped guard cells to estimate the influence of anatomical features on rapidity of responses.

Table 1 A summary of parameters referred to within the text with accompanying units

Parameter	Definition	Units
A	Net CO_2 assimilation rate	μmol m^{-2} s^{-1}
A_{95}	95% maximum A under 1000 μmol m^{-2} s^{-1} PPFD	μmol m^{-2} s^{-1}
C_a	Atmospheric CO_2 concentration	μmol mol^{-1}
C_i	Intracellular CO_2 concentration	μmol mol^{-1}
E	Water loss via transpiration	mol m^{-2} s^{-1}
GCW	Guard cell width	μm
g_s	Stomatal conductance to water vapour	mmol m^{-2} s^{-1}
G_{smax}	Predicted steady-state g_s under 1000 μmol m^{-2} s^{-1} PPFD	mmol m^{-2} s^{-1}
G_{smin}	Predicted steady-state g_s under 100 μmol m^{-2} s^{-1} PPFD	mmol m^{-2} s^{-1}
k	Time constant describing time taken to achieve steady-state g_s	min
k_i	Time constant for g_s to increase to G_{smax} under 1000 μmol m^{-2} s^{-1} PPFD	min
k_d	Time constant for g_s to decrease to steady-state under 100 μmol m^{-2} s^{-1} PPFD	min
PL	Stomatal pore length	μm
PPFD	Photosynthetically active photon flux density	μmol m^{-2} s^{-1}
SD	Stomatal density	mm^{-2}
SI_{max}	Maximum rate of g_s opening to an increase in PPFD from 100 to 1000 μmol m^{-2} s^{-1}	mmol m^{-2} s^{-1}
r_0	Minimum g_s of the sigmoidal response of g_s to a step increase in PPFD	mmol m^{-2} s^{-1}
VPD	Vapour pressure difference from leaf to air	kPa
W_i	Intrinsic water-use efficiency	μmol mol^{-1}
W_{i95}	W_i at A_{95}	μmol mol^{-1}
W_{imax}	Maximum W_i under 1000 μmol m^{-2} s^{-1} PPFD	μmol mol^{-1}
λ	Initial lag in the response time of g_s to a step increase in PPFD	min

Materials and Methods

Plant material and growth conditions

Thirteen important crop species (including three C_4 species) were selected along with the model plant *Arabidopsis thaliana,* and the relict gymnosperm species *Ginkgo biloba*. Eight had kidney- or elliptical-shaped guard cells whilst four had dumbbell-shaped guard-cells that are typically found in grasses.

Arabidopsis thaliana (Columbia, Col-0) seed was germinated in 100-cm^3 pots containing peat-based compost (Levingtons F2S, Everris, Ipswich, UK) and grown in a controlled environment (Reftech BV, Sassenheim, the Netherlands). Photosynthetic photon flux density (PPFD) was maintained at 155 ± 10 μmol m^{-1} s^{-1} for an 8 h photoperiod, whilst temperature and vapour pressure deficit (VPD) were 23°C and 1.1 kPa, respectively, day and night.

Oat (*Avena sativa*), sunflower (*Helianthus annuus*), tobacco (*Nicotiana tabacum*), pea (*Pisum sativum)*, tomato (*Solanum*

© 2016 The Authors
New Phytologist © 2016 New Phytologist Trust

lycopersicum), Sorgum (*Sorghum bicolor*), Barly (*Hordeum vulgare*), wheat (*Triticum aestivum*), maize (*Zea mays*), French bean (*Phaseolus vulgaris*) and broad bean (*Vicia faba*) were germinated in 650-cm^3 pots containing peat-based compost (Levington F2S). Following germination, plants were grown in a temperature-controlled glasshouse for 4–8 wk before measuring. Established Miscanthus (*Miscanthus nepalensis*) were supplied in 1-l pots from a commercial nursery (Beth Chatto, Colchester, UK). Solar radiation provided a PPFD of *c.* 500 μmol m^{-2} s^{-1}, supplemented by sodium vapour lamps (600W; Hortilux Schrèder, Monster, the Netherlands) to 300 μmol m^{-2} s^{-1} PPFD when external PPFD dropped below 1200 μmol m^{-2} s^{-1} over a 10 h period. Air temperature was maintained at 25°C ± 3°C during the day and 18°C ± 3°C at night. Plants were watered daily from below, with any excess water not absorbed by the pot within 2 h removed.

Rice (*Oryza sativa*) seeds were germinated and transferred to 650-cm^3 pots as described above and grown in a controlled environment with a photoperiod of 12 h : 12 h, light : dark at a PPFD of 500 ± 20 μmol m^{-2} s^{-1}, a day temperature of 25°C and VPD of 0.8 ± 0.2 kPa. Plants were measured after 12 wk.

Leaf gas-exchange measurements

Photosynthetic carbon assimilation (A) and stomatal conductance to water (g_s) were measured on the youngest fully expanded leaf using infrared gas analysis (Li-Cor 6400, Lincoln, NB, USA, and CIRAS-1, PP Systems, Amesbury, MA, USA). Light was provided by an integrated LED light source (Li-Cor, PP Systems). Leaves were first equilibrated at a PPFD of 100 μmol m^{-2} s^{-1} until both A and g_s reached 'steady state', this being defined as a < 2% change in rate during a 10-min period (*c.* 30–60 min). Once steady state was satisfied, PPFD was increased to 1000 μmol m^{-2} s^{-1} for 1 h before returning to 100 μmol m^{-2} s^{-1} for 30 min. The leaf cuvette was maintained at 400 μmol mol^{-1} CO_2 concentration (C_a), a leaf temperature of 20°C (±2°C) and a VPD of 1 ± 0.05 kPa. A and g_s were recorded every 1 min. Intrinsic water use efficiency (WUE) was calculated as $W_i = A/g_s$. All measurements were completed before 14:00 h to avoid any unwanted diurnal or circadian effects on photosynthesis.

Leaf anatomical measurements

Stomatal impressions of the ad- and abaxial leaf surfaces were taken of the same area, measured using gas exchange. A negative impression was made using a dental polymer (Xantoprene, Heraesus Kulzer Ltd, Hanau, Germany) following the methods of Weyers & Johansen (1985). Once the impression material had dried and was removed from the leaf, a positive impression was made from this by placing in nail varnish on a microscope slide. Stomatal density, guard cell length (L) and guard cell width were determined using ImageJ software (National Institute of Health, Bethesda, MD, USA) from twenty fields of view (size 1250 μm^2) captured from each impression using a 5 MP eye-piece camera (MicroCAM 5 MP, Bresser Optics, Rhede, Germany).

Modelling g_s, A and W_i responses to PPFD

In order to describe the temporal response of g_s to a single step-change in PPFD, an analytical model derived from the model by (Vialet-Chabrand *et al.*, 2013) was used (Fig. 1).

The model described the temporal response of g_s using a time constant (k, min), an initial time lag (λ, min) and a steady-state g_s (G_{smax}, mmol m^{-2} s^{-1}) reached at given PPFD:

$$g_s = (G_{smax} - r_0)e^{-e^{\left(\frac{\lambda - t}{k} + 1\right)}} + r_0 \qquad \text{Eqn 1}$$

(t, time, where time 0 is the point at which PPFD was increased from 100 to 1000 μmol m^{-2} s^{-1}; r_0 (mmol m^{-2} s^{-1}), initial value of stomatal conductance before the change in PPFD). In this equation, the time constant k is a measure of the rapidity of response of g_s independent of the amplitude of variation in g_s (Eqn 2). To distinguish between the time taken for the stomata to open (increase) and to close (decrease), the abbreviations k_i and k_d are used.

A second parameter combining rapidity and amplitude of the response, the maximum slope (Sl_{max}), was used to describe the maximal slope of the g_s response to the step-change in PPFD:

$$Sl_{max} = \frac{k.(G - r_0)}{e} \qquad \text{Eqn 2}$$

Parameter values were estimated using a Metropolis Hasting algorithm and a Bayesian model. The priors (*a priori* probability of the parameter values) used were uniform covering a large range of possible values and the initial values were chosen randomly. The initial values were chosen from observed values (± 10%) of both r_0 and G. For k, the range of values were selected from between 10 and 60 min, whilst λ values were between 0.1 and

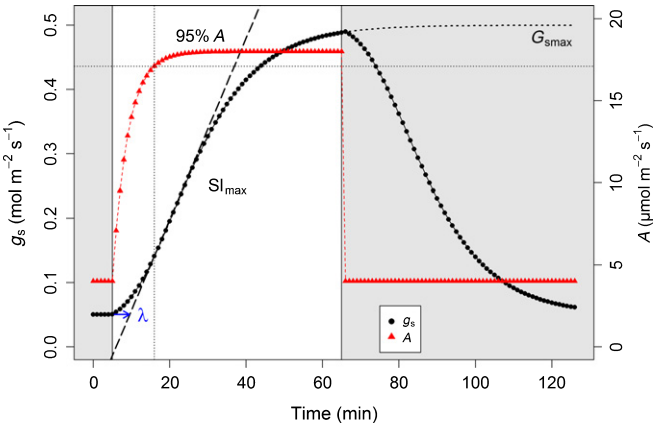

Fig. 1 Theoretical temporal response of stomatal conductance (g_s; black) and net CO_2 assimilation (A; red) to a step change in PPFD from 100 (shaded area) to 1000 (unshaded area) μmol m^{-2} s^{-1}. Where Sl_{max} describes the maximum temporal response of g_s (dashed line), λ describes the time-lag before g_s starts to increase (blue arrow) and G_{smax} describes the steady-state target of g_s under 1000 μmol m^{-2} s^{-1} PPFD. The dotted lines represented the time and the value were 95% A is reached.

© 2016 The Authors
New Phytologist © 2016 New Phytologist Trust

5 min. After 100 000 iterations using a thinning factor of 15, the chains were checked for stability and convergence (see Table 1).

Temporal responses in g_s limits A

During a step increase in PPFD, photosynthesis was considered limited by stomatal conductance until 95% A (A_{95}) was reached. Using this assumption, the percentage of limitation of A by g_s was estimated by:

$$\text{Limitation } (\%) = \frac{\int_0^t (A_{max} - A)}{\int_0^{60} A_{tot}} \quad \text{Eqn 3}$$

($\int_0^t (A_{max} - A)$, integral of the difference between the maximum potential A (A_{max}) and the observed limited A from the beginning of the observed curve to the time t where A reached 95% of the steady state; $\int_0^{60} A_{tot}$, maximum integral of A for 1 h period). Calculating the ratio using $\int_0^{60} A_{tot}$ normalized g_s limitation over the 1-h measurement period (see Table 1 for a summary of parameters).

The impact of different g_s and A responses on water loss

The nonsynchronous g_s and A response influences the temporal W_i response and the amount of water lost following a step increase in PPFD. To investigate the impact of g_s responses on water use efficiency, we predicted g_s from a simple model ($g_s = A/W_i$) using a constant W_i during the transient response. The constant value of W_i was chosen close to the maximum A (95%), assuming that this would be close to an optimal W_i with no limitation of A. On the one hand, when observed values of g_s were greater than predicted by the constant W_i model, more water was 'lost' than required to maintain optimal A; on the other, when observed values of g_s were lower than predicted, water was 'saved', illustrating a close coupling of g_s with A. As an investigating tool, this approach allowed us to assess the percentage of water 'lost' and 'saved' by comparing the coupling between A and g_s in different species.

Statistical analysis

Statistics were conducted using SPSS (v.16; SPSS Inc., Chicago, IL, USA) and R (http://www.r-project.org/). A Shapiro–Wilk test was used to test for normality and a Levene's test of homogeneity was used to determine if samples had equal variance. Single factor differences were analysed using a one-way ANOVA with a Tukey–Kramer honest significant difference test where more than one group existed or a Student's t-test where only two groups were compared.

Results

Most species measured achieved steady-state g_s after 60 min of high PPFD, except *Helianthus* and *Vicia*, which had not attained their maximum g_s values within this timeframe (Fig. 2), which might have led to an underestimation of their k_i values, which were already high (Fig. 3). Additionally, Ginkgo displayed atypical g_s and A behaviour (Fig. 2). The 30-min exposure to low light may not have been sufficient for complete, steady-state stomatal closure for some species; however, this does not greatly impact our estimations of additional water loss compared to instantaneous stomatal responses, because the major part of the water loss can be attributed to the initial rapid opening response of the stomata (Fig. 2).

Quantifying A and g_s responses to step changes in PPFD

Steady-state g_s at the initial PPFD of 100 μmol m^{-2} s^{-1} (G_{smin}) varied significantly among the species ($F_{(14,49)} = 5.007$, $P < 0.0001$), with the lowest values recorded for *G. biloba*

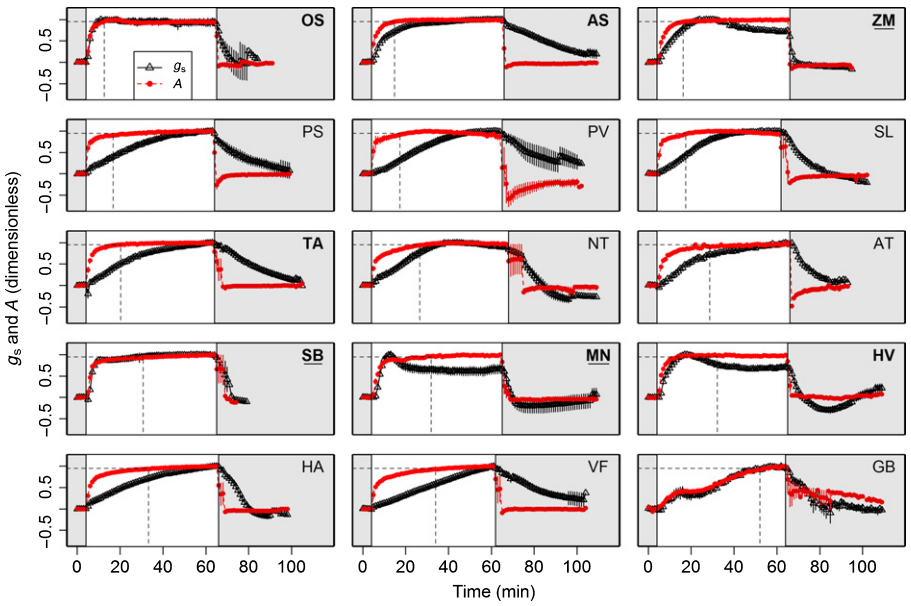

Fig. 2 Normalized temporal response of net CO_2 assimilation (A; circles) and stomatal conductance to water vapour (g_s; triangles) of 15 species to an increase in irradiance from 100 (shaded area) to 1000 (unshaded area) μmol m^{-2} s^{-1} followed by a decrease to 100 μmol m^{-2} s^{-1} (see Table 3 for abbreviations of species nomenclature). The dashed line indicates where 95% maximum A (A_{95}) was achieved. Data are the mean ± SE (n = 3–5). Values were normalized to the initial values at 100 μmol m^{-2} s^{-1} PPFD and maximum values at (1000 μmol m^{-2} s^{-1} PPFD).

© 2016 The Authors
New Phytologist © 2016 New Phytologist Trust

(13.2 mmol m^{-2} s^{-1}) and highest values for *T. aestivum* (255.9 mmol m^{-2} s^{-1}) (Fig. 3a; Supporting Information Fig. S1), whereas *A* was below 9 μmol m^{-2} s^{-1} for all species (Figs 3b, S2). An increase in PPFD to 1000 μmol m^{-2} s^{-1} led to an immediate and rapid increase in *A* compared to g_s for all species. After this initial period, the increase in *A* slowed to a magnitude similar to the concurrent increase in g_s. For the majority of species, *A* reached steady state while g_s continued to increase. These different periods of coupled and uncoupled responses of *A* and g_s were species-dependent. Although the majority of species displayed a mainly uncoordinated *A* and g_s temporal response (Fig. 2), final steady-state values of *A* and G_{smax} were significantly correlated among species ($r_{s(51)} = 0.78$, $P < 0.001$ for C_3 species and $r_{s(13)} = 0.84$, $P < 0.001$ for C_4 species – Fig. S3). In contrast to the majority of the species examined, *S. bicolor, O. sativa* and *G. biloba* all exhibited low g_s and an unusually strong coupling between *A* and g_s. The key difference between these three species was that *S. bicolor* and *O. sativa* exhibited a faster response of *A* and g_s, whereas *G. biloba* showed rather slower responses.

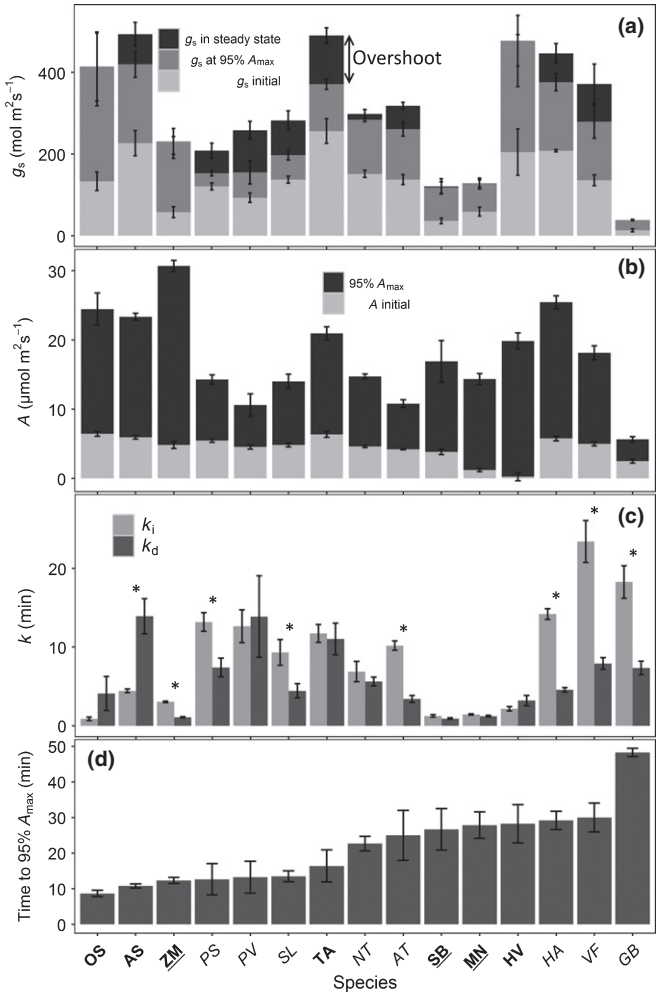

Fig. 3 Comparison between species of (a) steady-state g_s under 100 μmol m^{-2} s^{-1} PPFD (G_{smin}), g_s at 95% maximum net assimilation under 1000 μmol m^{-2} s^{-1} PPFD (A_{95}) and steady state (G_{smax}) under 1000 μmol m^{-2} s^{-1} PPFD for 15 species; (b) steady-state *A* under 100 μmol m^{-2} s^{-1} PPFD (*A* initial) and A_{95}; (c) time constants k_i and k_d for stomatal opening and closure, respectively; and (d) the time taken to reach A_{95}. Data are the mean ± SE ($n = 3$–5). Asterisks represented a significant asymmetry of k_i/k_d ($P < 0.05$). Species in bold have dumbbell-shaped guard cells, underlined species have a C_4 metabolism and species in plain font have elliptical-shaped guard cells and C_3 metabolism (see Table 3 for species name abbreviations).

The steady-state values of g_s (at 1000 μmol m^{-2} s^{-1} PPFD) estimated by the model (G_{smax}) were significantly different among species ($P < 0.0001$, $F_{(14,49)} = 14.469$; Fig. 3a), with observed values 10-fold higher in *T. aestivum* (482.9 ± 18.7 mmol m^{-2} s^{-1}) compared with *G. biloba* (45.2 ± 1.9 mmol m^{-2} s^{-1}). Values of G_{smax} were positively related to Sl_{max} ($r = 0.61$, $P < 0.01$) in elliptical- and dumbbell-shaped guard cells ($r = 0.41$, $P < 0.05$), whereas Sl_{max} was related to the total time taken to open to G_{smax} (k_i) in elliptical- ($r = -0.54$; $P < 0.01$) and dumbbell-shaped ($r = -0.68$; $P < 0.01$) guard cells (Table 2). Six out of the seven species with dumbbell-shaped guard cells showed the highest values of Sl_{max} (Table 3). Applying the Vialet–Chabrand model to the temporal response of g_s to an increase from 100 to 1000 μmol m^{-2} s^{-1} PPFD, showed that the initial lag time in the g_s response (λ) was significantly different among species ($P < 0.0001$, $F_{(14,49)} = 5.819$) and ranged from 12 s for *A. sativa* to 6 min for *G. biloba* (Table 3).

After PPFD was returned to 100 μmol m^{-2} s^{-1}, *A* decreased immediately whereas g_s showed a slow, exponential and species-dependent decrease. Most species showed a temporal response of g_s to decreasing light which was an order of magnitude lower than that of *A*, with some exceptions. *Sorghum bicolor* and *Z. mays* demonstrated significantly lower values of k_d (< 1 min; Fig. 3c) and thus faster responses compared to other species, approaching the speed of assimilation rate response to light (Fig. 2). When PPFD was returned to 100 μmol m^{-2} s^{-1}, no significant differences in λ were observed (data not shown), although steady-state g_s and Sl_{max} varied significantly amongst species.

Significant differences in the opening (k_i) and closing (k_d) time constants were observed amongst species (Fig. 3c); k_i ranged from 0.9 min in *O. sativa* to 23 min in *V. faba*, and k_d ranged from 0.9 min in *S. bicolor* to 14 min in *P. vulgaris*. k_i and k_d were positively correlated in species with elliptical- ($R^2 = 0.29$, $P < 0.01$) and dumbbell-shaped ($R^2 = 0.52$; $P < 0.001$) guard cells. Although the majority of species showed tendencies for greater rapidity in stomatal closing than opening (Fig. 3c), this was significant in only six species (Fig. 3c). On average, the species with dumbbell-shaped guard cells were 10 min faster in opening than elliptical species, reaching G_{smax} in significantly shorter periods of time ($t_{(44)} = -8.2$, $P > 0.0001$). C_4 species increased g_s more rapidly than C_3 species ($P < 0.0001$). Estimations from the closing response showed that dumbbell-shaped guard cells were also faster than elliptical-shaped guard cells ($P < 0.04$) and C_4 species closed faster than C_3 species ($P < 0.0001$) (Table 3).

g_s limitation of *A*

In order to assess the extent that *A* was limited by g_s during the increase of PPFD, we determined the time taken to reach 95% of

© 2016 The Authors
New Phytologist © 2016 New Phytologist Trust

Table 2 Correlation matrix between parameters (grey cells) describing the temporal response of g_s during opening and closing of elliptical- (upper triangle of the matrix) and dumbbell-shaped (lower triangle of the matrix) guard cells (see Table 3)

	Elliptical						
Dumbbell	Gs_{max}	ns	−0.48*	0.61**	0.47*	ns	ns
	ns	k_i	ns	−0.54**	ns	ns	ns
	ns	ns	λ	ns	ns	ns	ns
	0.41*	−0.42*	ns	SI_{max}	ns	0.47*	0.46*
	ns	ns	ns	ns	SD	ns	ns
	0.47**	0.72***	ns	ns	ns	PL	0.91***
	ns	ns	ns	ns	0.55**	−0.41*	GCW

	Elliptical						
Dumbbell	Gs_{max}	ns	ns	ns	ns	ns	ns
	0.44*	K_d	ns	0.68***	ns	ns	ns
	ns	0.49**	λ	ns	ns	ns	ns
	0.37*	0.62***	ns	SI_{max}	−0.68***	ns	ns
	ns	ns	ns	ns	SD	ns	ns
	0.6***	0.73***	ns	ns	ns	PL	0.91***
	ns	ns	ns	ns	0.55**	−0.41**	GCW

G_{smax}, predicted steady-state g_s under 1000 μmol m^{-2} s^{-1} PPFD; k_i, time constant for g_s to increase to G_{smax} under 1000 μmol m^{-2} s^{-1} PPFD; k_d, decrease from G_{smax} to G_{smin} under 100 μmol m^{-2} s^{-1}; λ, initial lag in the response time of g_s to a step increase in PPFD; SI_{max}, maximum rate of g_s opening to an increase in PPFD from 100 to 1000 μmol m^{-2} s^{-1}. Anatomical parameters of stomatal density (SD), pore length (PL) and guard cell width (GCW) were also compared. Significance: *, $P < 0.05$; **, $P < 0.01$; ***, $P < 0.001$; ns, not significant.

Table 3 Parameters of the dynamic model of g_s as estimated from a step increase in irradiance from 100 to 1000 μmol m^{-2} s^{-1} for 15 species

Species	Shape of guard cell/metabolism	Graph initials	K_i (min)	K_d (min)	λ (min)	SI_{max} (mmol m^{-2} s^{-2})	G (mmol m^{-2} s^{-1})
Oryza sativa	Dumbbell/C_3	OS	0.9 ± 0.21^{a}	4.1 ± 2.16^{abc}	0.11 ± 0.02^{a}	1.91 ± 0.60^{a}	424.50 ± 89.99^{abcd}
Sorghum bicolor	Dumbbell/C_4	SB	1.2 ± 0.16^{a}	0.9 ± 0.09^{a}	1.04 ± 0.17^{a}	0.46 ± 0.11^{bc}	118.32 ± 15.91^{ef}
Miscanthus nepalensis	Dumbbell/C_4	MN	1.4 ± 0.11^{a}	1.2 ± 0.10^{a}	1.36 ± 0.16^{ab}	1.56 ± 0.11^{bc}	175.56 ± 18.53^{ef}
Hordeum vulgare	Dumbbell/C_3	HV	2.2 ± 0.30^{a}	3.2 ± 0.70^{ab}	0.62 ± 0.37^{a}	1.01 ± 0.24^{ab}	529.07 ± 55.85^{a}
Zea mays	Dumbbell/C_4	ZM	3.0 ± 0.10^{ab}	1.1 ± 0.08^{a}	1.37 ± 0.23^{ab}	0.37 ± 0.02^{bc}	244.31 ± 33.18^{cdef}
Avena sativa	Dumbbell/C_3	AS	4.4 ± 0.23^{ab}	14.1 ± 2.37^{d}	0.20 ± 0.02^{a}	0.34 ± 0.03^{c}	478.95 ± 30.05^{ab}
Nicotiana tabacum	Elliptical/C_3	NT	6.9 ± 1.28^{abc}	6.5 ± 0.57^{abcd}	5.91 ± 1.39^{bc}	0.13 ± 0.01^{c}	316.21 ± 10.92^{bcde}
Solanum lycopersicum	Elliptical/C_3	SL	9.3 ± 1.64^{bcd}	4.4 ± 0.90^{abc}	3.27 ± 0.22^{abc}	0.10 ± 0.01^{c}	286.12 ± 22.78^{bcde}
Arabidopsis thaliana	Elliptical/C_3	AT	9.9 ± 0.69^{bcd}	3.4 ± 0.61^{abc}	1.0 ± 0.56^{ab}	0.11 ± 0.01^{c}	307.91 ± 8.69^{bcde}
Triticum aestivum	Dumb-bell/C_3	TA	11.7 ± 1.13^{cd}	11.8 ± 2.54^{cd}	1.03 ± 0.69^{a}	0.13 ± 0.02^{c}	482.98 ± 18.66^{ab}
Phaseolus vulgaris	Elliptical/C_3	PV	12.6 ± 2.08^{cde}	$11.4 \pm 6.10a^{bcd}$	3.75 ± 1.20^{abc}	0.10 ± 0.01^{c}	275.42 ± 23.58^{cde}
Pisum sativum	Elliptical/C_3	PS	13.2 ± 1.18^{cde}	7.9 ± 1.04^{abcd}	0.26 ± 0.03^{a}	0.04 ± 0.00^{c}	209.78 ± 18.34^{def}
Helianthus annuus	Elliptical/C_3	HA	14.2 ± 0.67^{de}	4.7 ± 0.35^{abc}	0.33 ± 0.03^{a}	0.09 ± 0.00^{c}	446.25 ± 25.52^{abc}
Ginkgo biloba	Elliptical/C_3	GB	18.3 ± 2.07^{ef}	7.3 ± 0.85^{abcd}	6.13 ± 2.53^{c}	0.01 ± 0.00^{c}	45.20 ± 9.10^{f}
Vicia faba	Elliptical/C_3	VF	23.4 ± 2.68^{f}	7.9 ± 0.75^{abcd}	0.29 ± 0.07^{a}	0.08 ± 0.02^{c}	430.14 ± 55.49^{abcd}

k_i and k_d, time constants for stomatal opening and closing, respectively; λ, initial lag time in response to an increase in irradiance; SI_{max}, maximum slope of the temporal response of g_s; G, steady-state target reached under 1000 μmol m^{-2} s^{-1} PPFD. The data are means ± SE ($n = 3$–8). Lowercase letters refer to significant differences ($P < 0.05$) between species (Tukey–Kramer honest significant difference). Species in bold have dumbbell-shaped guard cells, underlined species have a C_4 metabolism and species in plain font have elliptical-shaped guard cells and C_3 metabolism.

maximum A (A_{95}) at 1000 μmol m^{-2} s^{-1} PPFD (Fig. 3d). Further increases in g_s after A_{95} were substantially greater than the remaining 5% increase in A, suggesting that g_s was no longer limiting A (Fig. 2). Stomata opening did not increase significantly after A_{95} had been reached for the species with dumbbell-shaped guard cells (*Z. mays*, *S. bicolor*, *M. nepalensis*, *O. sativa*) and for *G. biloba* (Fig. 2). The majority of species achieved A_{95} within 30 min with values ranging between 5.7 and 30.7 μmol m^{-2} s^{-1} (Fig. 3b,d). *Zea mays* and *A. sativa* both attained the highest A and achieved A_{95} in the least time (12–11 min; Fig. 3d), whereas *G. biloba* was the slowest, taking on average 48 min to achieve the lowest A_{95}. Species with elliptical-shaped guard cells achieve significantly lower A_{95} ($P < 0.0001$) compared with species with dumbbell-shaped guard cells (Fig. 3b). The percentage of stomatal limitation of A during the opening response to A_{95} (Fig. 4) demonstrated significant variation among species ($P < 0.0001$, $F_{(14,49)} = 27.368$), with values ranging from 6.5 (*P. sativum*) to 24.3% (*G. biloba*). With the exception of *G. biloba*, which was statistically different from all other species, the limitation was 10–15%. Values of A_{95} also provided a set point from which to

© 2016 The Authors
New Phytologist © 2016 New Phytologist Trust

quantify the g_s response after A achieved near maximum steady state (Fig. 2, dotted line) with the majority of species with elliptical-shaped stomata showing an 'overshooting' in stomatal opening, demonstrated by a significant increase in g_s ($P < 0.01$) between 10 and 125 mmol m^{-2} s^{-1} (Fig. 3a). Species with dumbbell-shaped stomata (with the exception of *T. aestivum*; *A. sativa*) and *G. biloba* showed no or only a small 'overshoot' (< 3 mmol m^{-2} s^{-1} (Fig. 3a)).

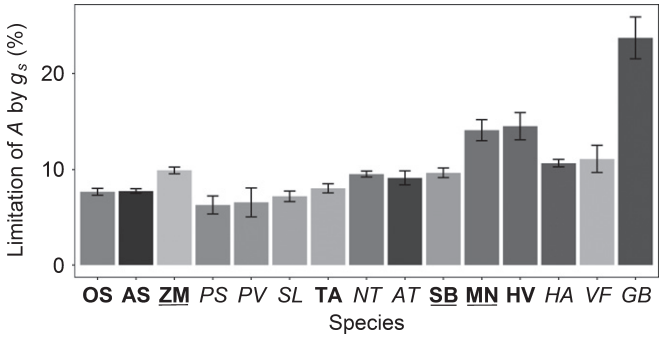

Fig. 4 Percentage limitation of net CO_2 assimilation (A) by stomatal conductance (g_s) after the 60 min at 1000 μmol m^{-2} s^{-1} PPFD. Data are the mean ± SE ($n = 3$–5). Species in bold have dumbbell-shaped guard cells, species underlined have a C_4 metabolism and species in plain font have elliptical guard cells and C_3 metabolism (see Table 3 for species name abbreviations).

Quantifying W_i responses to a step change in PPFD

The consequence of the lack of synchrony between the responses of A and g_s to a step increase in PPFD can be illustrated by the temporal responses of W_i (Figs 5, S4). Following the step increase in PPFD, A rapidly increased compared to g_s (Fig. 2) and W_i reached a maximum value (W_{imax}) well before A_{95} was achieved. The first 20 min of this response is shown in Fig. S4. The subsequent further increases in g_s drove a continuous decrease in W_i until both A and g_s reached steady state. In most of the C_3 species, W_i continued to decrease after A had reached a steady state due to the continued increase in g_s. W_{imax} represents the greatest CO_2 uptake for g_s; however, it should be noted that this value occurs earlier in the transient response before A_{95} is reached and that W_{imax} is achieved only for an extremely brief period of time. The diversity in W_i between species was determined by G_{smax} rather than A_{max} as no correlation between A_{max} with W_{imax} was observed, whereas G_{smax} was negatively correlated with W_{imax} ($P < 0.0001$, $r_s = -0.67$) and with W_i before the decrease in PPFD ($P < 0.0001$, $r_s = -0.74$). For example, *G. biloba*, *S. bicolour*, *M. nepalensis* and *Z. mays* achieved and maintained the highest W_i ($P < 0.001$) with vastly different values of A by maintaining a relatively low g_s compare to other species. The balance between CO_2 fixation and water loss was different between species, revealed by the four-fold difference in W_{imax} observed

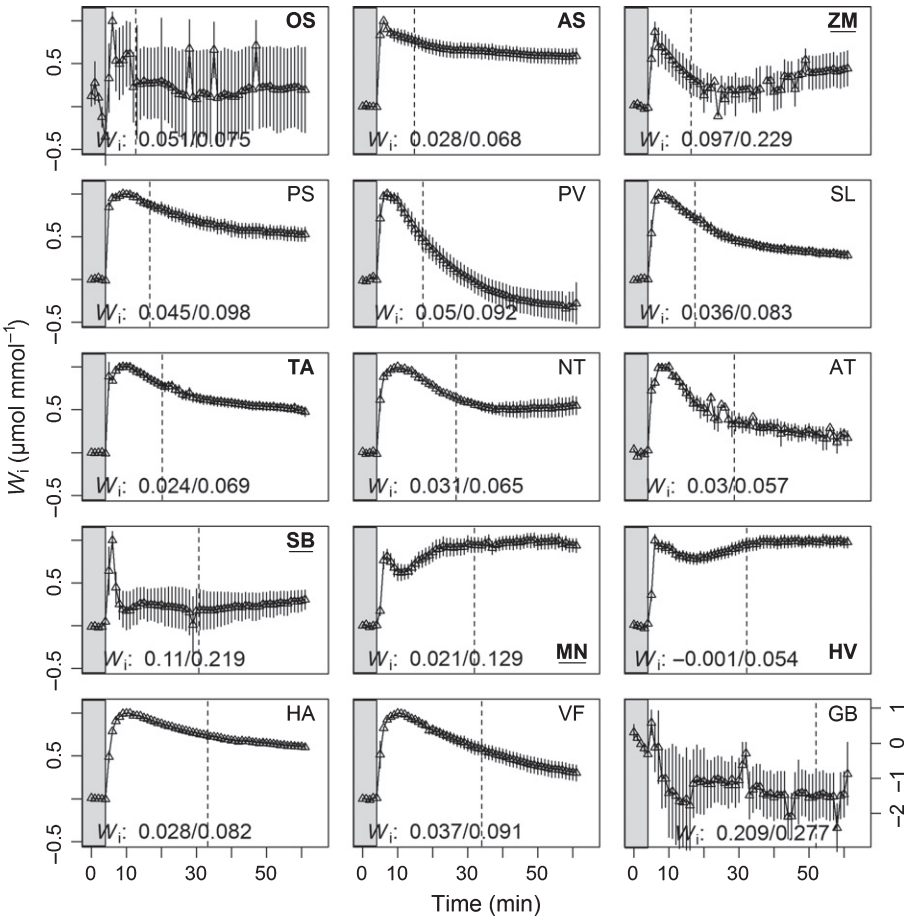

Fig. 5 Normalized temporal response of intrinsic water-use efficiency (W_i) of 15 species to an increase in irradiance from 100 (shade area) to 1000 (white area) μmol m^{-2} s^{-1}. Data are the mean ± SE ($n = 3$–5). The initial and maximal average values of W_i are indicated above the x-axis for each species and a dashed line denotes net CO_2 assimilation rate at 95% of maximum (A_{95}). Values were normalized to the initial values at 100 μmol m^{-2} s^{-1} PPFD and maximum values at (1000 μmol m^{-2} s^{-1} PPFD) (see Table 3 for species name abbreviations).

© 2016 The Authors
New Phytologist © 2016 New Phytologist Trust

between the 15 species, with the lowest values observed in *H. vulgare* (0.054 ± 0.006 µmol mmol^{-1} m^{-2} s^{-1}). On average, the percentage decrease between W_{imax} and W_i at the end of the response under 1000 µmol m^{-2} s^{-1} PPFD was significantly less in species with dumbbell-shaped guard cells ($P < 0.0001$) than in species with elliptical-shaped guard cells.

The temporal response of W_i is driven by the temporal variation in g_s to increasing PPFD that is uncoordinated with A, resulting in unnecessary water loss (Fig. 2). To investigate the theoretical variation of g_s required to optimize W_i, if coordinated with A, a model with a constant W_i chosen at A_{95} (W_{i95}) was applied and the difference between observed and modelled g_s assessed (Fig. 6), with modelled values of g_s greater than observed signifying 'water saving' and values less than observed representing a 'water loss'. Figure 6(a,b) show examples for *T. aestivum* and *V. faba*. During the first part of the response, the amount of potential 'water saved' was not significantly different between species (0.98–17.3%) (Fig. 6c). However, after W_{i95} was achieved, a significant difference in 'water loss' between species, in terms of percentage change in g_s ($P < 0.0001$, $F_{(14,49)} = 3.454$) was observed. For example, in *P. vulgaris*, g_s increased by 57% (± 23%) for only a 5% gain in A, which illustrates the strong uncoupling of A and g_s in this species and the negative impact on W_i (Figs 3a, S5). By contrast, the observed response of g_s in *S. bicolor* was close to the modelled optimal g_s with minimal increases in g_s once A_{95} was reached (Figs 3a, 6c).

The results revealed that W_{imax} and A_{95} were not reached at the same point during the temporal response (Fig. 5). To reach A_{95} (denoted by the dotted line, Fig. 5), the species typically displayed a decrease in W_i from W_{imax}. The percentage increase in A from 100 to 1000 µmol m^{-2} s^{-1} PPFD was significantly greater ($P < 0.01$) than the percentage decrease in W_i. The highest gains in A were observed for *G. biloba* and the species with dumbbell-shaped guard cells (with the exception of *M. nepalensis*) which all achieved > 30% increase in A (Fig. S5).

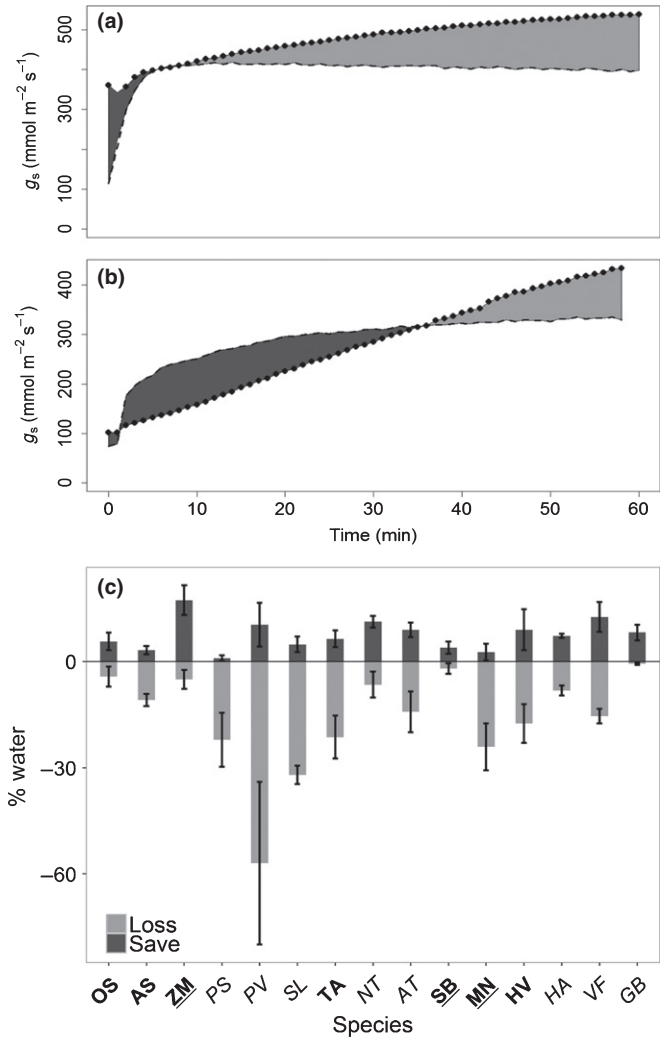

Fig. 6 Examples of observed (dotted lines) and modelled (dashed lines) temporal response of stomatal conductance to water vapour (g_s) for (a) wheat (*Triticum aestivum*) and (b) broad bean (*Vicia faba*). The modelled data represent g_s at constant water-use efficiency (W_i) achieved at 95% net CO_2 assimilation (A_{95}). The light grey shading represents water loss and the dark grey shading represents water conserved. (c) The percentage change in water loss (light grey) and water conserved (dark grey) for a 5% increase in A derived from the differences in observed and modelled for each species. Data are the mean ± SE ($n = 3$–5). Species in bold have dumbbell-shaped guard cells, underlined species have a C_4 metabolism and species in plain font have elliptical-shaped guard cells and C_3 metabolism (see Table 3 for species name abbreviations).

Anatomical features

Stomatal density was significantly different between species with abaxial stomatal densities ranging from 68.5 to 376.3 mm^{-2} and adaxial densities between 0 and 281.6 mm^{-2} (Fig. S6) A positive correlation between ad- and abaxial density for species both with elliptical- ($R^2 = 0.87$) and dumbbell-shaped ($R^2 = 0.79$ excluding *M. nepalenis*) guard cells was observed. When considering both types of guard cells, a strong correlation between abaxial and adaxial values for stomatal density ($R^2 = 0.76$ excluding *M. nepalensis*), pore length (PL; $R^2 = 0.79$) and guard cell width (GCW; $R^2 = 0.85$) was also observed, and therefore mean values were used to correlate with stomatal response traits. A strong correlation between PL and GCW was observed and hence only PL was used for further analyses.

With reference to opening responses of elliptical-shaped guard cells, no significant relationships were found between the anatomical features (PL and SD) and Sl_{max}, k or G, whereas in dumbbell-shaped guard cells, PL and SD correlated significantly with G_{smax}, and k_i was correlated with PL but not with SD. The same correlations were observed with reference to closing responses in both guard cell types; however, a significant relationship between SD and k_i was also observed in dumbbell-shaped guard cells (Table 2).

Discussion

As light changes rapidly and is often considered the most dynamic and most important environmental variable influencing both stomatal behaviour and photosynthetic rate, we examined the kinetics of photosynthesis (A) and stomatal conductance (g_s)

© 2016 The Authors
New Phytologist © 2016 New Phytologist Trust

to a step increase followed by a decrease in photosynthetic photon flux density (PPFD), in a number of species; assessing the speeds of the g_s response, the amplitude of change, g_s limitation of A and the impact of these kinetics on intrinsic water use efficiency (W_i). The temporal dynamics showed clear species-specific differences and noncoordination between A and g_s, with g_s exhibiting a slower and more varied response than A. Such uncoordinated A and g_s responses could have significant implications for cumulative carbon assimilation and transpirational water loss, especially in dynamic light environments. For example, Lawson & Blatt (2014) modelled synchronous g_s and A behaviour and calculated a theoretical 20% increase in water use efficiency if g_s responded instantaneously to the changes in PPFD and matched mesophyll demands for CO_2.

A combination of rapid responses and high steady-state values of g_s reduce CO_2 diffusional limitations of A, but can also drastically reduce W_i, due to the nonlinear relationship between A and g_s (Wong *et al.*, 1979). We show for example that the high steady-state values and rapid responses observed in *Oryza sativa*, *Avena sativa* and *Triticum aestivum* facilitated high photosynthetic rates but ultimately resulted in low W_i, which may be indicative of traditional breeding and selection practices for high yield at the expense of water loss (Jones, 1987). Although high g_s reduces W_i, it is also possible that, under well-watered conditions, such stomatal behaviour would increase overall photosynthetic carbon gain by enabling plants to opportunistically use sun flecks in the canopy that can occur on a timescale of seconds to hours (Chazdon & Pearcy, 1991; Kirschbaum *et al.*, 1988; Pearcy, 1990; Way & Pearcy, 2012). Under the measurement conditions used here, when PPFD was raised A immediately (within 1 min) increased in all species, indicating that g_s at the lower light level was greater than required. However, a clear stomatal limitation of A was also apparent as all species took > 9 min to reach 95% final A (A_{95}) (Fig. 3d).

A common feature of g_s dynamics was the noncoordination in A and g_s responses and the continued stomatal opening after A_{95} had been reached (or 'overshooting' of g_s; Fig. 3a), resulting in decreases in W_i. The observed diversity in responses of A and g_s in the species measured questions the mechanisms that coordinate these parameters. Intercellular CO_2 concentration (C_i) was originally proposed as the mediator for the close correlation between g_s and A (Wong *et al.*, 1979; Farquhar & Wong, 1984; Mansfield *et al.*, 1990; Buckley *et al.*, 2003). It was assumed that stomata adjust to a steady-state aperture to maintain C_i at 2/3 atmospheric [CO_2] (Ehleringer & Pearcy, 1983) and therefore, when A is increasing the resulting decrease in C_i would cause stomata to open and *vice versa*. When A reaches steady state, further increases in g_s would result in a greater C_i that cannot increase A and therefore, following the C_i hypothesis, no further increases in g_s would be expected once steady-state A has been achieved. However, our results do not fully support this conclusion (e.g. *Vicia faba* in Fig. 2) and agree with findings from work on transgenic plants with reductions in photosynthesis, which showed increasing g_s with light despite high C_i (Von Caemmerer *et al.*, 2004; Baroli *et al.*, 2008; Lawson *et al.*, 2008). Many studies support C_i-driven stomatal responses (e.g. Roelfsema & Prins, 1995) and we do not argue against CO_2 as a driver; however, our results show that C_i is clearly not of high priority in the hierarchy.

Stomata have been a key target for improving plant water use efficiency (WUE) and/or a plant's ability to cope with reductions in water availability. However, improvements of WUE in crop plants often come at the expense of photosynthetic rates (Yoo *et al.*, 2009, 2010) and are therefore of limited value, given that current global research efforts focus on increasing crop yield for sustainable food and fuel production (Long *et al.*, 2015). However, as we have illustrated here, W_{imax} does not correspond to maximum assimilation rate (Fig. 5) as maximum WUE can often only be achieved when g_s restricts A. Based on these observations of dynamic responses we could suggest a steady-state g_s target that would provide a compromise between A and W_i and propose that this target should be the lowest g_s value that enables A_{95} to be achieved. It should be noted that this is an optimal target and that fluctuations in the environment could result in different integrated values of A, g_s and therefore W_i, highlighting the importance of appreciating the speed of stomatal responses and coordination between A and g_s.

It is well known that significant variation in photosynthetic capacity (A_{max}) exists both within and amongst different species (Lawson *et al.*, 2012) and, as observed here, this is generally correlated with steady-state g_s (and G_{smax}). As may be expected the C_4 species measured in our study were able to achieve a greater A_{95} at a lower g_s (at A_{95}) compared to C_3 species (Fig. S3), and it is likely that the faster stomatal opening and closing responses observed in C_4 species (Fig. 3c) facilitated this greater level of coordination between A and g_s (Fig. 2). This faster response was a common feature not just in C_4 plants, but also C_3 species with dumbbell-shaped guard cells. However, despite the close coupling in C_4 species, the same stomatal limitation on A of *c.* 10% or greater was observed in both C_4 and C_3 plants (Fig. 4). This illustrates the importance of considering both CO_2 uptake and water loss when evaluating steady-state or transient W_i (McAusland *et al.*, 2013), as maximum W_i is often not observed at maximum A. Here the decrease in W_i (between W_{imax} and A_{95}) with increasing g_s was outweighed by a substantial gain in A in all species.

The temporal uncoupling between stomatal behaviour and carbon demand observed in many species can be evaluated by comparing measured g_s responses with those modelled assuming a stable W_i (at A_{95}, which represented a W_i value that is achieved without a limitation on A), providing an estimate of the differences between variable and stable W_i in terms of water gain and expense for each species. Using this model over the period measured, stomatal behaviour in the majority of species resulted in water expense exceeding water conservation, illustrating that the latter was not the priority. As all the plants in these experiments were maintained under relatively well-watered conditions, this would have led to a higher stomatal conductance than would be observed in plants experiencing water limitation (Comstock & Ehleringer, 1993; Mott & Peak, 2012; Lawson & Blatt, 2014). In general, C_4 species were an exception to this and either demonstrated a balanced water budget or greater gains than

© 2016 The Authors
New Phytologist © 2016 New Phytologist Trust

losses, further exemplifying the more synchronous A and g_s responses observed in the three species measured. The most likely explanation for the greater loss of water in C_3 species is the substantial overshoot in g_s after A_{95} had been achieved, which was not apparent in the two C_4 species studied (Figs 3a, 6).

However, C_3 species with rapid stomata responses (e.g. *O. sativa*) also exhibited a positive water balance, whilst species with the slowest stomatal opening (with the exception of *G. biloba*) demonstrated the most negative water balances (Fig. 6c) hinting at the possible existence interspecific diversity of stomatal control.

The rapidity of response for stomata to open (increase; k_i) and close (decrease; k_d) was positively correlated for species with elliptical- as well as dumbbell-shaped guard cells, suggesting that similar mechanisms or pathways were involved in both opening and closing responses. Overall, significant asymmetry of the stomatal responses revealed a faster closing than opening, which has previously been associated with conserving water (Tinoco-Ojanguren & Pearcy, 1993; Ooba & Takahashi, 2003). In comparison, species with dumbbell-shaped guard cells displayed the fastest responses and most had greater similarity in the rapidity of opening and closing, which is consistent with the fact that these guard cells require fewer solutes and less water to achieve a given unit increase in aperture (Franks & Farquhar, 2007; Raven, 2014). The rapidity of increasing g_s impacts on A, with species with high k_i taking longer to achieve A_{95}, as low g_s restricts CO_2 diffusion. Under field conditions with a dynamic light environment, slowly responding stomata could restricted CO_2 uptake and thus have a compound effect on the cumulative A over the growing season and affect yield (Reynolds *et al.*, 1994; Fischer *et al.*, 1998). However, slow stomatal closure would negatively impact on W_i when environmental conditions reduce A. It should be noted that under field conditions, changing the light environment also results in changes in leaf temperature. A direct impact of increasing PPFD would be an increased leaf temperature, which would lead to higher leaf-to-air vapour pressure difference and thus exacerbate the transpirational losses of 'overshooting' stomata. However, higher transpirational losses would have a cooling effect. Therefore, concomitant temperature variation could have complex effects on the dynamic responses of A, g_s and W_i, and should be studied in detail using appropriate experimental set-ups.

Variation between species was also observed in the maximum speed of g_s response (Sl_{max}) and the rapidity of opening (k_i) to achieve steady-state conductance. Previous research has associated the speed of stomatal responses with the size of stomata, with smaller stomata facilitating rapid opening and closing (Hetherington & Woodward, 2003; Franks & Farquhar, 2007; Franks & Beerling, 2009; Drake *et al.*, 2013; Raven, 2014).The majority of these studies have used the maximum slope (Sl_{max}) as a measure of the maximum speed of response; however, this measurement is also dependent on the amplitude of the response (Eqn 2). Additionally, because g_s is determined by both stomatal aperture and density, small changes in aperture in plants with smaller, more numerous stomata will have a greater Sl_{max} for the same change in aperture as species with fewer larger stomata. Therefore, although Sl_{max} may provide a useful comparative measure within species (in which anatomical features and the scales of stomatal responses are similar), it is not a useful parameter to compare speeds of response between species with different anatomical features and magnitudes of change. To address this issue, we used the time constant k to provide a measure of the rapidity of g_s, independently of the magnitude of response and the absolute g_s values observed. For elliptical-shaped guard cells, we did not detect any significant correlation between stomatal density and Sl_{max} or k, suggesting that on an interspecific basis neither the speed nor the amplitude of the stomatal responses to PPFD were dependent on stomatal density. On the other hand, for dumbbell-shaped guard cells, variation among species in stomatal size impacted on the speed and amplitude of stomatal responses. This hints at the possibility that for elliptical-shaped guard cells attributes other than anatomical features are important contributors to the speed of stomatal responses (Hetherington & Woodward, 2003; Franks & Beerling, 2009) such as membrane permeability due to ion channels number or distribution (see discussion, Lawson & Blatt, 2014). By contrast, for dumbbell-shaped guard cells, anatomical variations seem to impact the rapidity of their response. Additionally, these species were also able to achieve a greater Sl_{max} and tended to be faster. This may be due to the energetic requirements for stomatal movement of the often smaller dumbbell-shaped guard cells (Grantz & Assmann, 1991; Franks & Farquhar, 2007; Raven, 2014). The dumbbell-shaped design means that small changes in width can cause larger changes in stomatal aperture and maximize the potential of these stomata to track changes in environmental conditions (Hetherington & Woodward, 2003).

Although transients of leaf-level W_i provide insight into potentially optimizing stomatal behaviour, numerous other processes contribute to W_i in the field. Manipulation of the speed of g_s provides scope for improving carbon acquisition in fluctuating light environments but also enhances drought tolerance through improved conservation of water. Integration of these dynamic responses over daily or seasonal time periods is complex and would require a model that includes respiration (both from leaves and parts including stems and roots) and transpiration as a product of changes in diurnal saturation deficit (Cowan & Farquhar, 1977; Farquhar *et al.*, 1989; Jones, 2004) Identifying varieties or genotypes with more rapid stomatal responses could be used as an optimizing strategy for whole-plant water use over the growing period, potentially improving the ability of the plant to adapt to changing environments (Schulze & Hall, 1982; Campitelli *et al.*, 2016) which could feed forward to maintain or improve yields (Chaerle *et al.*, 2005; Lawson & Blatt, 2014).

Conclusion

This is one of the few studies to investigate temporal responses in A and g_s in relation to carbon assimilation and W_i, and illustrates significant species-specific variation in the speed of stomatal responses and magnitude of change, as well as coordination with A. Slow stomatal responses can limit A by *c.* 10%, which could equate to substantial losses in photosynthetic rates, productivity

© 2016 The Authors
New Phytologist © 2016 New Phytologist Trust

and reductions in yield. Previous research focusing on improving productivity has shown that by enhancing photosynthesis by only 2–3%, substantial increases in plant growth and biomass can be achieved over the season (Lefebvre *et al.*, 2005; Zhu *et al.*, 2007; Simkin *et al.*, 2015). The work presented here illustrates that similar short-term improvements in A could be gained by improving the rapidity of stomatal responses and coordination with A. Tighter coupling between stomata and A therefore has the potential to achieve a substantial improvement in WUE, as in the present study, overshooting of g_s by up to 80% was observed for only a 5% gain in A and fast closing responses resulted in substantial saving in water loss.

Our findings support faster responses in dumbbell- compared with elliptical-shaped guard cells and suggest that photosynthetic type (C_3/C_4) also plays a role. The speed of stomatal responses might not be dependent on the same underlying processes when comparing elliptic- and dumbbell-shaped guard cells, with physiological processes being more important for the former and anatomical features for the latter. Improving the rapidity of stomatal responses could greatly improve productivity and W_i but achieving this will require greater knowledge of the physiological and molecular mechanisms that determine the speed of stomata and coordination with mesophyll demands for CO_2, and further field-based measurements that integrate the dynamics of A, g_s and W_i over seasons.

Acknowledgements

NERC funding is acknowledged for PhD studentship to L.M. (NERC quota studentship). S.V-C. was supported by a BBSRC grant BB/1001187_1 to T.L. We are also grateful to Sue Corbett for her help in the glasshouse.

Author contributions

L.M., N.R.B. and T.L. planned and designed the research. L.M., S.V-C., P.D. and T.L. performed experiments and analysed data, L.M., S.V-C., P.D., N.R.B., O.B. and T.L. wrote the manuscript.

References

Assmann SM, Wang XQ. 2001. From milliseconds to millions of year: guard cells and environmental responses. *Current Opinion in Plant Biology* **4**: 421–428.

Baroli I, Price GD, Badger MR, Von Caemmerer S. 2008. The contribution of photosynthesis to the red light response of stomatal conductance. *Plant Physiology* **146**: 737–747.

Blum A. 2009. Effective use of water (EUW) and not water-use efficiency (WUE) is the target of crop yield improvement under drought stress. *Field Crops Research* **112**: 119–123.

Buckley T, Mott K, Farquhar G. 2003. A hydromechanical and biochemical model of stomatal conductance. *Plant, Cell & Environment* **26**: 1767–1785.

Campitelli BE, Des Marais DL, Juenger TE. 2016. Ecological interactions and the fitness effect of water-use efficiency: competition and drought alter the impact of natural MPK12 alleles in Arabidopsis. *Ecology letters* **19**: 424–434.

Chaerle L, Saibo N, Van Der Straeten D. 2005. Tuning the pores: towards engineering plants for improved water use efficiency. *Trends in Biotechnology* **23**: 308–315.

Chazdon RL, Pearcy RW. 1991. The importance of sunflecks for forest understory plants. *BioScience* **41**: 760–766.

Comstock J, Ehleringer J. 1993. Stomatal response to humidity in common bean (*Phaseolus vulgaris*): implications for maximum transpiration rate, water-use efficiency and productivity. *Functional Plant Biology* **20**: 669–691.

Condon A, Rebetzke R, Farquhar G. 2002. Improving intrinsic water-use efficiency and crop yield. *Crop Science* **42**: 122.

Cowan I, Farquhar G. 1977. Stomatal function in relation to leaf metabolism and the environment. In: Jennings DH, ed. *Integration of activity in the higher plants; Symposia of the Society of Experimental Biology*. Cambridge, UK: Cambridge University Press, 471–505.

Drake PL, Froend RH, Franks PJ. 2013. Smaller, faster stomata: scaling of stomatal size, rate of response, and stomatal conductance. *Journal of Experimental Botany* **64**: 495–505.

Ehleringer J, Pearcy RW. 1983. Variation in quantum yield for CO_2 uptake among C_3 and C_4 plants. *Plant Physiology* **73**: 555–559.

Farquhar GD, Ehleringer JR, Hubick KT. 1989. Carbon isotope discrimination and photosynthesis. *Annual Review of Plant Biology* **40**: 503–537.

Farquhar GD, Sharkey TD. 1982. Stomatal conductance and photosynthesis. *Annual Review of Plant Biology* **33**: 317–345.

Farquhar G, Wong S. 1984. An empirical model of stomatal conductance. *Functional Plant Biology* **11**: 191–210.

Fischer R, Rees D, Sayre K, Lu Z-M, Condon A, Saavedra AL. 1998. Wheat yield progress associated with higher stomatal conductance and photosynthetic rate, and cooler canopies. *Crop Science* **38**: 1467–1475.

Franks PJ, Beerling DJ. 2009. Maximum leaf conductance driven by CO_2 effects on stomatal size and density over geologic time. *Proceedings of the National Academy of Sciences, USA* **106**: 10 343–10 347.

Franks PJ, Farquhar GD. 2007. The mechanical diversity of stomata and its significance in gas-exchange control. *Plant Physiology* **143**: 78–87.

Grantz D, Assmann S. 1991. Stomatal response to blue light: water use efficiency in sugarcane and soybean. *Plant, Cell & Environment* **14**: 683–690.

Hetherington AM, Woodward FI. 2003. The role of stomata in sensing and driving environmental change. *Nature* **424**: 901–908.

Jones HG. 1987. *Breeding for stomatal characters*. Stanford, CA, USA: Stanford University Press.

Jones HG. 1998. Stomatal control of photosynthesis and transpiration. *Journal of Experimental Botany* **49**: 387–398.

Jones HG. 2004. *What is water use efficiency?* Oxford, UK: Blackwell Publishing.

Knapp AK, Smith WK. 1987. Stomatal and photosynthetic responses during sun/shade transitions in subalpine plants: influence on water use efficiency. *Oceologica* **74**: 62–67.

Knapp AK, Smith WK. 1990. Stomatal and photosynthetic responses to variable sun light. *Physiologica Plantarum* **78**: 160–165.

Lawson T, Blatt M. 2014. Stomatal size, speed and responsiveness impact on photosynthesis and water use efficiency. *Plant Physiology* **164**: 1556–1570.

Lawson T, Caemmerer S, Baroli I. 2010. Photosynthesis and Stomatal Behaviour. *Progress in Botany* **72**: 265–304.

Lawson T, Kramer DM, Raines CA. 2012. Improving yield by exploiting mechanisms underlying natural variation of photosynthesis. *Current Opinion in Biotechnology* **23**: 215–220.

Lawson T, Lefebvre S, Baker NR, Morison JI, Raines CA. 2008. Reductions in mesophyll and guard cell photosynthesis impact on the control of stomatal responses to light and CO_2. *Journal of Experimental Botany* **59**: 3609–3619.

Leakey A, Scholes J, Press M. 2005. Physiological and ecological significance of sunflecks for dipterocarp seedlings. *Journal of Experimental Botany* **56**: 469–482.

Lefebvre S, Lawson T, Fryer M, Zakhleniuk OV, Lloyd JC, Raines CA. 2005. Increased sedoheptulose-1,7-bisphosphatase activity in transgenic tobacco plants stimulates photosynthesis and growth from an early stage in development. *Plant Physiology* **138**: 451–460.

Long SP, Marshall-Colon A, Zhu X-G. 2015. Meeting the global food demand of the future by engineering crop photosynthesis and yield potential. *Cell* **161**: 56–66.

Mansfield T, Hetherington A, Atkinson C. 1990. Some current aspects of stomatal physiology. *Annual Review of Plant Biology* **41**: 55–75.

© 2016 The Authors
New Phytologist © 2016 New Phytologist Trust

McAusland L, Davey P, Kanwal N, Baker N, Lawson T. 2013. A novel system for spatial and temporal imaging of intrinsic plant water use efficiency. *Journal of Experimental Botany* **64**: 4993–5007.

Mott KA, Peak D. 2012. Testing a vapour-phase model of stomatal responses to humidity. *Plant, Cell & Environment* **36**: 936–944.

Naumburg E, Ellsworth DS, Katul GG. 2001. Modeling dynamic understory photosynthesis of contrasting species in ambient and elevated carbon dioxide. *Oecologia* **126**: 487–499.

Ooba M, Takahashi H. 2003. Effect of asymmetric stomatal response on gas-exchange dynamics. *Ecological Modelling* **164**: 65–82.

Pearcy RW. 1990. Sunflecks and photosynthesis in plant canopies. *Annual Review of Plant Biology* **41**: 421–453.

Raven JA. 2014. Speedy small stomata? *Journal of Experimental Botany* **65**: 1415–1424.

Reynolds M, Balota M, Delgado M, Amani I, Fischer R. 1994. Physiological and morphological traits associated with spring wheat yield under hot, irrigated conditions. *Functional Plant Biology* **21**: 717–730.

Roelfsema MRG, Prins H. 1995. Effect of abscisic acid on stomatal opening in isolated epidermal strips of abi mutants of *Arabidopsis thaliana. Physiologia Plantarum* **95**: 373–378.

Schulze E-D, Hall A. 1982. Stomatal responses, water loss and CO_2 assimilation rates of plants in contrasting environments. In: Lange OL, Nobel PS, Osmond CB, Ziegler H, eds. *Physiological plant ecology II.* Berlin: Springer, 181–230.

Simkin AJ, McAusland L, Headland LR, Lawson T, Raines CA. 2015. Multigene manipulation of photosynthetic carbon assimilation increases CO_2 fixation and biomass yield in tobacco. *Journal of Experimental Botany* **66**: 4075–4090.

Tinoco-Ojanguren C, Pearcy RW. 1993. Stomatal dynamics and its importance to carbon gain in two rainforest *Piper* species. *Oecologia* **94**: 395–402.

Vialet-Chabrand S, Dreyer E, Brendel O. 2013. Performance of a new dynamic model for predicting diurnal time courses of stomatal conductance at the leaf level. *Plant, Cell & Environment* **36**: 1529–1546.

Vico G, Manzoni S, Palmroth S, Katul G. 2011. Effects of stomatal delays on the economics of leaf gas exchange under intermittent light regimes. *New Phytologist* **192**: 640–652.

Von Caemmerer S, Lawson T, Oxborough K, Baker NR, Andrews TJ, Raines CA. 2004. Stomatal conductance does not correlate with photosynthetic capacity in transgenic tobacco with reduced amounts of Rubisco. *Journal of Experimental Botany* **55**: 1157.

Way DA, Pearcy RW. 2012. Sunflecks in trees and forests: from photosynthetic physiology to global change biology. *Tree Physiology* **32**: 1066–1081.

Weyers JD, Johansen LG. 1985. Accurate estimations of stomatal aperture from silicon rubber impressions. *New Phytologist* **10**: 109–115.

Wong S, Cowan I, Farquhar G. 1979. Stomatal conductance correlates with photosynthetic capacity. *Nature* **282**: 424–426.

Yoo CY, Pence HE, Hasegawa PM, Mickelbart MV. 2009. Regulation of transpiration to improve crop water use. *Critical Reviews in Plant Science* **28**: 410–431.

Yoo CY, Pence HE, Jin JB, Miura K, Gosney MJ, Hasegawa PM, Mickelbart MV. 2010. The Arabidopsis GTL1 transcription factor regulates water use efficiency and drought tolerance by modulating stomatal density via transrepression of SDD1. *Plant Cell Online* **22**: 4128.

Zhu X-G, de Sturler E, Long SP. 2007. Optimizing the distribution of resources between enzymes of carbon metabolism can dramatically increase photosynthetic rate: a numerical simulation using an evolutionary algorithm. *Plant Physiology* **145**: 513–526.

Supporting Information

Additional Supporting Information may be found online in the Supporting Information tab for this article:

Fig. S1 Response of stomatal conductance to water vapour (g_s) of 15 species to an increase in irradiance from 100 to 1000 μmol m^{-2} s^{-1} PPFD.

Fig. S2 Response of net CO_2 assimilation (A) of 15 species to an increase in irradiance from 100 to 1000 μmol m^{-2} s^{-1} PPFD.

Fig. S3 The relationship between 95% maximum net CO_2 assimilation (A_{95}) and steady-state stomatal conductance under 1000 μmol m^{-2} s^{-1} PPFD (G_{smax}) for 15 species.

Fig. S4 Normalized temporal response of intrinsic water-use efficiency (W_i) of 15 species for the first 20 min after an increase in irradiance from 100 to 1000 μmol m^{-2} s^{-1}.

Fig. S5 Determining the percentage decrease in intrinsic water-use efficiency (W_i) for a percentage increase in CO_2 assimilation (A) between maximum W_i max to 95% of the maximum A (A_{95}) reached under 1000 μmol m^{-2} s^{-1} PPFD for 15 species.

Fig. S6 Counts of stomatal density and measurements of guard cell length and width for 15 species from the adaxial and abaxial surfaces of the leaf.

Please note: Wiley Blackwell are not responsible for the content or functionality of any supporting information supplied by the authors. Any queries (other than missing material) should be directed to the *New Phytologist* Central Office.

© 2016 The Authors
New Phytologist © 2016 New Phytologist Trust